Proceedings of the ASME 2010 International Mechanical Engineering Congress & Exposition
IMECE2010
November 12-18, 2010, Vancouver, British Columbia, Canada

IMECE2010-38437

ROBUST GAIN-SCHEDULED CONTROL OF A UAV BASED ON A POLYTOPIC MODEL APPROXIMATION

Juan A. Ramirez
Dept. of Mechanical Engineering
Universidad Pontificia Bolivariana
P.O. Box 56006
Medellín, Colombia
juan.ramirezm@correo.upb.edu.co

Luis B. Gutierrez
Dept. of Electrical Engineering
Universidad Pontificia Bolivariana
P.O. Box 56006
Medellín, Colombia
lbgutie@ieee.org

Rafael E. Vasquez*
Dept. of Mechanical & Aerospace Engineering
University of Florida
P.O. Box 116300
Gainesville, Florida 32611
revasquez@ufl.edu*

ABSTRACT

This work addresses the design of a robust $\mathcal{H}_\infty$ gain-scheduled controller for the Condor Andino UAV (Unmanned Aerial Vehicle). A polytopic approximation of the linearization family of the nonlinear model is used for the design. Because the linearization family in the operating region derives in a linear parameter varying (LPV) description with a nonlinear dependence of a set of parameters, a least squares approximation of the system matrices is used in order to obtain affine dependence. The polytopic description is obtained from the affine LPV model when the operating range is defined choosing the varying parameter inside a convex hull. The controller is synthesized using the Bounded Real Lemma in order to guarantee quadratic $\mathcal{H}_\infty$ performance over the operating region. The simulation results show that the designed controller can be successfully applied to the nonlinear system over the operating range.

Keywords: Gain Scheduling; $\mathcal{H}_\infty$; Polytopic Systems; Robust Control; UAV.

INTRODUCTION

The Automation and Design Research Group A+D from the Universidad Pontificia Bolivariana (Medellín, Colombia) has been developing the fixed-wing unmanned aerial vehicle Condor Andino, Fig. 1. The development process includes the design, construction, integration and test of the mechanical/electrical elements and the design, simulation and implementation of the control system which allows autonomous and radio-controlled flights. The vehicle has double tail-boom, 5-meter wingspan and is powered by a BT-64 EI Fuji pusher engine with a 22-in diameter and 10-in pitch two-blade propeller.

Several advances have been made in the mechanical/aeronautical design [1], hardware and software architecture [2], modeling [3], simulation [4] and navigation [5] of the UAV. For the control system, a three-level architecture is used, based on the ideas shown in [6, 7]: at high-level the mission planner designs the trajectory in terms of a set of feasible waypoints, at mid-level the guidance system takes the waypoints and calculates filtered setpoints and, at low-level the controller follows the setpoints using the vehicle's state estimation and manipulating the control inputs. The design of the low-level control strategy is an open problem and several solutions can be used, from simple-linear to complex-nonlinear strategies. Some available gain-scheduled robust $\mathcal{H}_\infty$ design techniques can be used [8–10]. These techniques search for linear-parameter-varying (LPV) gain-scheduled controllers able to quadratically stabilize a plant over an operation region, holding some $\mathcal{H}_\infty$ performance of the exogenous inputs - controlled variables map [11, 12].

In this work, the controller synthesis is achieved using a polytopic approximation of the Jacobian linearization family of the plant's nonlinear model [13]. The problem can be expressed as a finite number of linear matrix inequalities (LMIs) and solved using available software tools [14, 15].

*Address all correspondence to this author.

FIGURE 1. CONDOR ANDINO UAV

DESIGN METHOD

The controller design methodology is based on the work of Apkarian et al. [9]. They propose a robust $\mathcal{H}_\infty$ controller for a class of linear-parameter-varying (LPV) plants given by the state–space model

$$\begin{aligned}\dot{x} &= \mathrm{A}(\sigma(t))\,x + \mathrm{B}(\sigma(t))\,u,\\ y &= \mathrm{C}(\sigma(t))\,x + \mathrm{D}(\sigma(t))\,u;\end{aligned} \tag{1}$$

where x is the state, y is the output, u is the input and σ is a time-varying parameter. The state–space matrices A, B, C and D are properly dimensioned and depend affinely on σ. This means that they can be written as

$$\begin{aligned}A(\sigma) &= M_{A0} + \sum_{i=1}^{\mathrm{p}} \sigma_i M_{Ai}, \quad B(\sigma) = M_{B0} + \sum_{i=1}^{\mathrm{p}} \sigma_i M_{Bi},\\ C(\sigma) &= M_{C0} + \sum_{i=1}^{\mathrm{p}} \sigma_i M_{Ci}, \quad D(\sigma) = M_{D0} + \sum_{i=1}^{\mathrm{p}} \sigma_i M_{Di};\end{aligned} \tag{2}$$

where $\sigma = \begin{bmatrix}\sigma_1 & \sigma_2 & \cdots & \sigma_{\mathrm{p}}\end{bmatrix}^{\mathrm{T}}$. The parameter σ is assumed to vary inside a convex polytope of vertices ω_i, $i = 1,\ldots,\mathrm{r}$; thus σ is defined by the convex combination

$$\begin{aligned}\sigma \in \Theta &= \mathrm{Co}\{\omega_1, \omega_2, \ldots, \omega_{\mathrm{r}}\}\\ &= \left\{\sum_{i=1}^{\mathrm{r}} \mu_i \omega_i; \mu_i \geq 0; \sum_{i=1}^{\mathrm{r}} \mu_i = 1\right\}.\end{aligned} \tag{3}$$

If Eqns. (2) and (3) hold, then A, B, C and D can be written as a convex combination and define the polytope of matrices

$$\begin{aligned}\begin{bmatrix}A(\sigma) & B(\sigma)\\ C(\sigma) & D(\sigma)\end{bmatrix} \in \wp = \mathrm{Co}&\left\{\begin{bmatrix}A_i & B_i\\ C_i & D_i\end{bmatrix} = \begin{bmatrix}A(\omega_i) & B(\omega_i)\\ C(\omega_i) & D(\omega_i)\end{bmatrix}\right\}\\ &= \left\{\sum_{i=1}^{\mathrm{r}} \mu_i \begin{bmatrix}A_i & B_i\\ C_i & D_i\end{bmatrix} : \mu_i \geq 0, \sum_{i=1}^{\mathrm{r}} \mu_i = 1\right\}.\end{aligned} \tag{4}$$

Plants defined by Eqn. (1) holding (4) are called polytopic. A more general description of the system in Eqn. (1) is

$$\begin{aligned}\dot{x} &= \mathrm{A}(\sigma)\,x + \mathrm{B}_1(\sigma)\,w + \mathrm{B}_2(\sigma)\,u,\\ z &= \mathrm{C}_1(\sigma)\,x + \mathrm{D}_{11}(\sigma)\,w + \mathrm{D}_{12}(\sigma)\,u,\\ y &= \mathrm{C}_2(\sigma)\,x + \mathrm{D}_{21}(\sigma)\,w + \mathrm{D}_{22}(\sigma)\,u;\end{aligned} \tag{5}$$

where z are controlled outputs, y are measured outputs, u are control inputs and w are exogenous inputs.

The design problem for plants represented by Eqn. (5) consists in finding an LPV controller

$$\begin{aligned}\dot{x}_{\mathrm{K}} &= \mathrm{A_K}(\sigma(t))\,x_{\mathrm{K}} + \mathrm{B_K}(\sigma(t))\,y,\\ u &= \mathrm{C_K}(\sigma(t))\,x_{\mathrm{K}} + \mathrm{D_K}(\sigma(t))\,y;\end{aligned} \tag{6}$$

which ensures $\mathcal{H}_\infty$ quadratic performance. This means that for the closed-loop mapping from w to z shown in Fig. 2

$$\begin{aligned}\dot{\mathrm{x}} &= \mathrm{A_{cl}}(\sigma)\,\mathrm{x} + \mathrm{B_{cl}}(\sigma)\,w,\\ z &= \mathrm{C_{cl}}(\sigma)\,\mathrm{x} + \mathrm{D_{cl}}(\sigma)\,w;\end{aligned} \tag{7}$$

where x is the complete state, the following statements are true for all possible σ in Θ:

(A1) there exists a single quadratic Lyapunov function $V(\mathrm{x}) = \mathrm{x}^{\mathrm{T}} X \mathrm{x}$ such that $\mathrm{A_{cl}}$ is stable;

(A2) the $\mathcal{H}_\infty$ norm of the mapping from w to z is bounded by some scalar γ

$$\left\|\mathrm{D_{cl}}(\sigma) + \mathrm{C_{cl}}(\sigma)\,(sI - \mathrm{A_{cl}}(\sigma))^{-1}\,\mathrm{B_{cl}}(\sigma)\right\|_\infty < \gamma \tag{8}$$

and the $\mathcal{L}_2$ norm is bounded by $\|z\|_2 \leq \gamma \|w\|_2$.

If such LPV controller (6) exists and σ is measurable, the controller is self-scheduled with respect to σ and guarantees global stability for all arbitrary σ trajectories in Θ, [9].

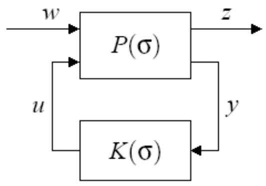

FIGURE 2. CLOSED-LOOP LPV SYSTEM

Through the Bounded Real Lemma conditions, (A1) and (A2) are true if for all σ in Θ, the LMI

$$\begin{bmatrix} \mathrm{A}_{\mathrm{cl}}^{\mathrm{T}}(\sigma)X + X\mathrm{A}_{\mathrm{cl}}(\sigma) & X\mathrm{B}_{\mathrm{cl}}(\sigma) & \mathrm{C}_{\mathrm{cl}}^{\mathrm{T}}(\sigma) \\ \mathrm{B}_{\mathrm{cl}}^{\mathrm{T}}(\sigma)X & -\gamma I & \mathrm{D}_{\mathrm{cl}}^{\mathrm{T}}(\sigma) \\ \mathrm{C}_{\mathrm{cl}}(\sigma) & \mathrm{D}_{\mathrm{cl}}(\sigma) & -\gamma I \end{bmatrix} < 0 \tag{9}$$

holds. The problem in Eqn. (9) requires solving a LMI with infinite number of constraints. This problem can be reduced to a finite set of LMIs if the closed-loop system is polytopic.

The problem is solvable if the following conditions hold:

(B1) the mapping between the control input u and the controlled variables z is zero *i.e.* $D_{12}(\sigma) = 0$;
(B2) matrices $B_2(\sigma) = B_2$, $C_2(\sigma) = C_2$, $D_{12}(\sigma) = D_{12}$, $D_{21}(\sigma) = D_{21}$ are parameter independent;
(B3) the pairs $(A(\sigma), B_2)$ and $(A(\sigma), C_2)$ are quadratically stabilizable and detectable for all σ respectively.

Condition (B1) is necessary for well-posedness of the loop but can often be removed by redefining the plant output and condition (B3) is necessary for the existence of a stabilizing controller (6). Condition (B2) is necessary for the closed-loop system to be polytopic so the problem can be solved using a finite number of LMIs. This condition can be checked if the closed-loop matrices are written as

$$\begin{aligned} \mathrm{A}_{\mathrm{cl}}(\sigma) &= \mathrm{A}_0(\sigma) + \mathcal{B}(\sigma)K(\sigma)\mathcal{C}(\sigma), \\ \mathrm{B}_{\mathrm{cl}}(\sigma) &= \mathrm{B}_0(\sigma) + \mathcal{B}(\sigma)K(\sigma)\mathcal{D}_{21}(\sigma), \\ \mathrm{C}_{\mathrm{cl}}(\sigma) &= \mathrm{C}_0(\sigma) + \mathcal{D}_{12}(\sigma)K(\sigma)\mathcal{C}(\sigma), \\ \mathrm{D}_{\mathrm{cl}}(\sigma) &= \mathrm{D}_{11}(\sigma) + \mathcal{D}_{12}(\sigma)K(\sigma)\mathcal{D}_{21}(\sigma); \end{aligned} \tag{10}$$

where

$$\begin{aligned} \mathrm{A}_0(\sigma) &= \begin{bmatrix} \mathrm{A}(\sigma) & 0 \\ 0 & 0_{k\times k} \end{bmatrix}, & \mathrm{B}_0(\sigma) &= \begin{bmatrix} \mathrm{B}_1(\sigma) \\ 0 \end{bmatrix}, \\ \mathrm{C}_0(\sigma) &= \begin{bmatrix} \mathrm{C}_1(\sigma) & 0 \end{bmatrix}, & \mathcal{B}(\sigma) &= \begin{bmatrix} 0 & \mathrm{B}_2 \\ I_k & 0 \end{bmatrix}, \\ \mathcal{C}(\sigma) &= \begin{bmatrix} 0 & I_k \\ \mathrm{C}_2 & 0 \end{bmatrix}, & \mathcal{D}_{12}(\sigma) &= \begin{bmatrix} 0 & \mathrm{D}_{12} \end{bmatrix}, \\ \mathcal{D}_{21}(\sigma) &= \begin{bmatrix} 0 \\ \mathrm{D}_{21} \end{bmatrix}, & K(\sigma) &= \begin{bmatrix} \mathrm{A_K}(\sigma) & \mathrm{B_K}(\sigma) \\ \mathrm{C_K}(\sigma) & \mathrm{D_K}(\sigma) \end{bmatrix}; \end{aligned}$$

and k is the controller order. It can be seen in Eqn. (10) that in order to have an LPV-polytopic controller and polytopic plant at the same time, matrices $\mathcal{B}$, $\mathcal{C}$, $\mathcal{D}_{12}$, $\mathcal{D}_{21}$ must be parameter independent *i.e.* constant matrices.

If $\mathrm{B}_2(\sigma)$ and/or $\mathrm{C}_2(\sigma)$ are parameter dependent, the open-loop plant can be augmented by pre-filtering and/or post-filtering the control input u and/or the measured variable y by defining a new control input $\tilde{u}$ and a new measured output $\tilde{y}$

$$\begin{aligned} \dot{x}_u &= A_u x_u + B_u \tilde{u}, \\ u &= C_u x_u, \\ \dot{x}_y &= A_y x_y + B_y y, \\ \tilde{y} &= C_y x_y; \end{aligned} \tag{11}$$

so the augmented open-loop plant is given by

$$\begin{aligned} \begin{bmatrix} \dot{x} \\ \dot{x}_u \\ \dot{x}_y \end{bmatrix} &= \begin{bmatrix} \mathrm{A}(\sigma) & \mathrm{B}_2(\sigma)C_u & 0 \\ 0 & A_u & 0 \\ B_y\mathrm{C}_2(\sigma) & 0 & A_y \end{bmatrix} \begin{bmatrix} x \\ x_u \\ x_y \end{bmatrix} \\ &+ \begin{bmatrix} \mathrm{B}_1(\sigma) \\ 0 \\ B_y\mathrm{D}_{21}(\sigma) \end{bmatrix} w + \begin{bmatrix} 0 \\ B_u \\ 0 \end{bmatrix} \tilde{u}, \end{aligned} \tag{12}$$

$$z = \begin{bmatrix} \mathrm{C}_1(\sigma) & \mathrm{D}_{12}(\sigma)C_u & 0 \end{bmatrix} \begin{bmatrix} x \\ x_u \\ x_y \end{bmatrix} + \mathrm{D}_{11}(\sigma)w, \tag{13}$$

$$y = \begin{bmatrix} 0 & 0 & C_y \end{bmatrix} \begin{bmatrix} x \\ x_u \\ x_y \end{bmatrix}. \tag{14}$$

When conditions (B1) – (B3) hold, using convexity, Eqn. (9) is equivalent to the system of inequalities

$$\begin{bmatrix} \mathrm{A}_{\mathrm{cl}i}^{\mathrm{T}}X + X\mathrm{A}_{\mathrm{cl}i} & X\mathrm{B}_{\mathrm{cl}i} & \mathrm{C}_{\mathrm{cl}i}^{\mathrm{T}} \\ \mathrm{B}_{\mathrm{cl}i}^{\mathrm{T}}X & -\gamma I & \mathrm{D}_{\mathrm{cl}i}^{\mathrm{T}} \\ \mathrm{C}_{\mathrm{cl}i} & \mathrm{D}_{\mathrm{cl}i} & -\gamma I \end{bmatrix} < 0, \quad i = 1,\ldots,\mathrm{r}; \tag{15}$$

where $\mathrm{A}_{\mathrm{cl}i}$, $\mathrm{B}_{\mathrm{cl}i}$, $\mathrm{C}_{\mathrm{cl}i}$ and $\mathrm{D}_{\mathrm{cl}i}$ are the images of the vertices ω_i.

In Eqn. (15) there are $\mathrm{r}+1$ unknown matrices i.e. X and K_i, $i = 1,\ldots,\mathrm{r}$, so the problem is not linear in X and K_i. As shown in [9], the existence of a controller guaranteeing quadratic $\mathcal{H}_\infty$ can be established if there exist two symmetric matrices R and S satisfying the $2\mathrm{r}+1$ LMIs

$$\left[\begin{array}{c|c} \mathcal{N}_R & 0 \\ \hline 0 & I \end{array}\right]^{\mathrm{T}} \left[\begin{array}{cc|c} \mathrm{A}_i R + R\mathrm{A}_i^{\mathrm{T}} & R\mathrm{C}_{1i}^{\mathrm{T}} & \mathrm{B}_{1i} \\ \mathrm{C}_{1i}R & -\gamma I & \mathrm{D}_{11i} \\ \hline \mathrm{B}_{1i}^{\mathrm{T}} & \mathrm{D}_{11i}^{\mathrm{T}} & -\gamma I \end{array}\right] \left[\begin{array}{c|c} \mathcal{N}_R & 0 \\ \hline 0 & I \end{array}\right] < 0, \quad i = 1,2,\ldots,\mathrm{r}; \tag{16}$$

$$\left[\begin{array}{c|c}\mathcal{N}_S & 0\\ \hline 0 & I\end{array}\right]^{\mathrm{T}}\left[\begin{array}{cc|c}\mathrm{A}_iS+S\mathrm{A}_i^{\mathrm{T}} & S\mathrm{B}_{1i} & \mathrm{C}_{1i}^{\mathrm{T}}\\ \mathrm{B}_{1i}^{\mathrm{T}}S & -\gamma I & \mathrm{D}_{11i}^{\mathrm{T}}\\ \hline \mathrm{C}_{1i} & \mathrm{D}_{11i} & -\gamma I\end{array}\right]\left[\begin{array}{c|c}\mathcal{N}_S & 0\\ \hline 0 & I\end{array}\right]<0, \tag{17}$$
$$i=1,2,\ldots,\mathrm{r};$$

$$\begin{bmatrix} R & I\\ I & S\end{bmatrix}\geq 0; \tag{18}$$

where $\mathcal{N}_R$ is the base of the null space of $\begin{bmatrix} B_2^{\mathrm{T}} & D_{12}^{\mathrm{T}}\end{bmatrix}$ and $\mathcal{N}_S$ is the base of the null space of $\begin{bmatrix} C_2 & D_{21}\end{bmatrix}$. Furthermore, there exists a polytopic controller $\mathrm{K}(\sigma)$ of order k if and only if R and S satisfy the rank constraint

$$\mathrm{rank}(I-RS)\leq k. \tag{19}$$

Therefore, from R and S we need to find complete rank matrices M, N satisfying

$$MN^{\mathrm{T}}=I-RS. \tag{20}$$

Then, X is the unique solution of the matrix equation $\Pi_2 = X_{\mathrm{cl}}\Pi_1$, where

$$\Pi_1=\begin{bmatrix} S & I\\ N^T & 0\end{bmatrix}, \Pi_2=\begin{bmatrix} I & R\\ 0 & M^T\end{bmatrix}.$$

Finally, if X is known (and fixed), the vertex controllers K_i can be calculated from Eqn. (15) since these inequalities now appear as r LMIs in K_i.

AIRCRAFT MODEL

Two different models of the aircraft's dynamics are used, one for simulation and one for control design. The simulation model used to test the controllers is a complete model that considers the rigid-body dynamics, the nonlinear behavior of aerodynamic forces and moments, and a blade element theory model of the thrust forces and moments in the propeller. The model used in the control design process is a reduced model that only considers the uncoupled longitudinal/lateral dynamics of the aircraft. Both models use the following nomenclature:

- m is the mass and J_x, J_y, J_z, J_{xz} are the moments and products of inertia, and $\Gamma = J_xJ_z - J_{xz}^2$;
- ϕ, θ, ψ are the roll, pitch and yaw Euler's angles respectively;
- α, β are the angle of attack and sideslip angle respectively;
- U, V, W are the body frame $x-y-z$ velocity components;
- p, q, r are the roll, pitch and yaw angular rates respectively;
- D, Y, L are the drag, crossforce and lift forces respectively;
- l, m, n are the roll, pitch and yaw moments;
- T is the thrust force;
- τ_m is the propeller's torque;
- ω_m is the propeller's angular speed;
- J_p is the propeller/motor's moment of inertia; and
- g is the acceleration due to gravity.

The simulation model uses flat-earth dynamic equations defined in the body frame [16] given by

$$\begin{aligned}\dot{U} =& \frac{1}{\mathrm{m}}\left(-D\cos\alpha\cos\beta - Y\cos\alpha\sin\beta + L\sin\alpha + T\right)\\ & -g\sin\theta - \left(qW-rV\right),\end{aligned} \tag{21}$$

$$\dot{V} = \frac{1}{\mathrm{m}}\left(-D\sin\beta + Y\cos\beta\right) + g\sin\phi\cos\theta - \left(rU-pW\right), \tag{22}$$

$$\begin{aligned}\dot{W} =& \frac{1}{\mathrm{m}}\left(-D\sin\alpha\cos\beta - Y\sin\alpha\sin\beta - L\cos\alpha\right)\\ & +g\cos\phi\cos\theta - \left(pV-qU\right),\end{aligned} \tag{23}$$

$$\begin{aligned}\dot{p} =& \frac{1}{\Gamma}\left[\left(J_z\mathrm{c}\alpha + J_{xz}\mathrm{s}\alpha\right)\left(l\mathrm{c}\beta - m\mathrm{s}\beta\right) - \left(J_z\mathrm{s}\alpha + J_{xz}\mathrm{c}\alpha\right)n\right.\\ & -\left(J_z\left(J_z-J_y\right)+J_{xz}^2\right)qr + J_{xz}\left(J_x-J_y+J_z\right)pq\\ & \left.+J_z\tau_m + J_{xz}J_pq\omega_m\right],\end{aligned} \tag{24}$$

$$\begin{aligned}\dot{q} =& \frac{1}{J_y}\left[l\mathrm{s}\beta + m\mathrm{c}\beta + \left(J_z-J_x\right)pr - J_{xz}\left(p^2-r^2\right)\right.\\ & \left.-J_pr\omega_m\right],\end{aligned} \tag{25}$$

$$\begin{aligned}\dot{r} =& \frac{1}{\Gamma}\left[\left(J_z\mathrm{s}\alpha + J_{xz}\mathrm{c}\alpha\right)\left(l\mathrm{c}\beta - m\mathrm{s}\beta\right) - \left(J_{xz}\mathrm{s}\alpha - J_x\mathrm{c}\alpha\right)n\right.\\ & -\left(J_x\left(J_x-J_y\right)+J_{xz}^2\right)pq - J_{xz}\left(J_x-J_y+J_z\right)qr\\ & \left.+J_{xz}\tau_m + J_xJ_pq\omega_m\right];\end{aligned} \tag{26}$$

The kinematic equations are given by

$$\dot{\phi} = p + q\tan\theta\sin\phi + r\tan\theta\cos\phi, \tag{27}$$

$$\dot{\theta} = q\cos\phi - r\sin\phi, \tag{28}$$

$$\dot{\psi} = q\frac{\sin\phi}{\cos\theta} + r\frac{\cos\phi}{\cos\theta}. \tag{29}$$

The translational dynamic equations used in controller design are defined in the wind frame, *i.e.* using V_T, α and β instead of U, V and W, assuming zero wind velocity. Let us define

$$\begin{bmatrix} V_T\\ \alpha\\ \beta\end{bmatrix} = \begin{bmatrix}\sqrt{U^2+V^2+W^2}\\ \mathrm{atan2}\left(W,U\right)\\ \mathrm{atan2}\left(V,\sqrt{U^2+W^2}\right)\end{bmatrix}. \tag{30}$$

Then, taking the time-derivative of Eqn. (30) and substituting into Eqns. (21) - (23) yields

$$\begin{aligned} \mathrm{m}\dot{V}_T =& -D + T\mathrm{c}\alpha\mathrm{c}\beta \\ & + \mathrm{m}g\left(-\mathrm{c}\alpha\mathrm{c}\beta\mathrm{s}\theta + \mathrm{s}\beta\mathrm{s}\phi\mathrm{c}\theta + \mathrm{s}\alpha\mathrm{c}\beta\mathrm{c}\phi\mathrm{c}\theta\right), \end{aligned} \tag{31}$$

$$\begin{aligned} \mathrm{m}\mathrm{c}\beta V_T\dot{\alpha} =& -L - T\mathrm{s}\alpha + \mathrm{m}g\left(\mathrm{s}\alpha\mathrm{s}\theta + \mathrm{c}\alpha\mathrm{c}\phi\mathrm{c}\theta\right) \\ & + \mathrm{m}V_T\left(q\mathrm{c}\beta - \left(p\mathrm{c}\alpha + r\mathrm{s}\alpha\right)\mathrm{s}\beta\right), \end{aligned} \tag{32}$$

$$\begin{aligned} \mathrm{m}V_T\dot{\beta} =& Y - T\mathrm{c}\alpha\mathrm{s}\beta \\ & + \mathrm{m}g\left(\mathrm{c}\alpha\mathrm{s}\beta\mathrm{s}\theta + \mathrm{c}\beta\mathrm{s}\phi\mathrm{c}\theta - \mathrm{s}\alpha\mathrm{s}\beta\mathrm{c}\phi\mathrm{c}\theta\right) \\ & - \mathrm{m}V_T\left(r\mathrm{c}\alpha - p\mathrm{s}\alpha\right). \end{aligned} \tag{33}$$

As mentioned, the uncoupled equations are defined in the longitudinal and lateral modes: the longitudinal mode assumes that $\beta \equiv p \equiv r \equiv \phi \equiv 0$ and the lateral mode assumes that $\dot{V}_T \equiv \dot{\alpha} \equiv q \equiv 0$. Thus, the longitudinal dynamics equations obtained from (31), (32), (25), and (28) are given by

$$\mathrm{m}\dot{V}_T = -D + T\cos\alpha + \mathrm{m}g\left(-\cos\alpha\sin\theta + \sin\alpha\cos\theta\right) \tag{34}$$

$$\begin{aligned} \mathrm{m}V_T\dot{\alpha} =& -L - T\sin\alpha + \mathrm{m}g\left(\sin\alpha\sin\theta + \cos\alpha\cos\theta\right) \\ & + \mathrm{m}V_T q, \end{aligned} \tag{35}$$

$$\dot{q} = \frac{m}{J_y}, \tag{36}$$

$$\dot{\theta} = q, \tag{37}$$

$$\dot{h} = V_T\left(\cos\alpha\sin\theta - \sin\alpha\cos\theta\right), \tag{38}$$

and the lateral dynamics equations obtained from (33), (24), (26), (27), and (29) are given by

$$\begin{aligned} \mathrm{m}V_{T0}\dot{\beta} =& Y - T_0\mathrm{c}\alpha_0\mathrm{s}\beta \\ & + \mathrm{m}g\left(\mathrm{c}\alpha_0\mathrm{s}\beta\mathrm{s}\theta_0 + \mathrm{c}\beta\mathrm{s}\phi\mathrm{c}\theta_0 - \mathrm{s}\alpha_0\mathrm{s}\beta\mathrm{c}\phi\mathrm{c}\theta_0\right) \\ & - \mathrm{m}V_{T0}\left(r\mathrm{c}\alpha_0 - p\mathrm{s}\alpha_0\right), \end{aligned} \tag{39}$$

$$\begin{aligned} \dot{p} =& \frac{1}{\Gamma}\left[\left(J_z\mathrm{c}\alpha_0 + J_{xz}\mathrm{s}\alpha_0\right)\left(l\mathrm{c}\beta - m_0\mathrm{s}\beta\right)\right. \\ & \left. - \left(J_z\mathrm{s}\alpha_0 + J_{xz}\mathrm{c}\alpha_0\right)n + J_z\tau_m\right], \end{aligned} \tag{40}$$

$$\begin{aligned} \dot{r} =& \frac{1}{\Gamma}\left[\left(J_z\mathrm{s}\alpha_0 + J_{xz}\mathrm{c}\alpha_0\right)\left(l\mathrm{c}\beta - m_0\mathrm{s}\beta\right)\right. \\ & \left. - \left(J_{xz}\mathrm{s}\alpha_0 - J_x\mathrm{c}\alpha_0\right)n + J_{xz}\tau_m\right], \end{aligned} \tag{41}$$

$$\dot{\phi} = p + r\tan\theta_0\cos\phi, \tag{42}$$

$$\dot{\psi} = r\frac{\cos\phi}{\cos\theta_0}. \tag{43}$$

Equations (34) to (43) can be used to obtain two space-state models, one for each mode. For the longitudinal mode

$$\begin{aligned} \dot{x}_{\text{long}} &= f_{\text{long}}(x_{\text{long}}, u_{\text{long}}), \\ y_{\text{long}} &= \left[\, V_T \;\; h \;\; \theta - \alpha \;\; q \,\right]^{\mathrm{T}}, \end{aligned} \tag{44}$$

with $x_{\text{long}} = \left[\, V_T \;\; \alpha \;\; q \;\; \theta \;\; h \,\right]^T$ and $u_{\text{long}} = \left[\, \delta_\omega \;\; \delta_E \,\right]^T$; and for the lateral mode

$$\begin{aligned} \dot{x}_{\text{lat}} &= f_{\text{lat}}(x_{\text{lat}}, u_{\text{lat}}), \\ y_{\text{lat}} &= \left[\, \psi \;\; \beta \;\; r \;\; \phi \;\; p \,\right]^{\mathrm{T}}, \end{aligned} \tag{45}$$

with $x_{\text{lat}} = \left[\, \beta \;\; p \;\; r \;\; \phi \;\; \psi \,\right]^T$ and $u_{\text{lat}} = \left[\, \delta_A \;\; \delta_R \,\right]^T$.

POLYTOPIC APPROXIMATION

An LPV model can be obtained from a parametrization of the linearization family of the nonlinear models (44) and (45), and the linearization family is obtained for the set of steady-level flight quasi-equilibrium points *i.e.* points that satisfy the condition

$$\dot{V}_T = \dot{\alpha} = \dot{\theta} = q = \dot{h} = \beta = p = r = \dot{\psi} = 0,$$

subject, from Eqns. (44) and (45), to

$$\begin{aligned} f_{\text{long}}(x_{\text{long}}, u_{\text{long}}) &= 0, \\ f_{\text{lat}}(x_{\text{lat}}, u_{\text{lat}}) &= 0, \end{aligned} \tag{46}$$

respectively [13]. A general form for the input and state equilibrium values of the longitudinal and lateral modes is

$$\begin{aligned} x_{\text{long}e} &= \left[\, V_{T0} \;\; \alpha_0 \;\; 0 \;\; \alpha_0 \;\; h_0 \,\right]^{\mathrm{T}}, \\ u_{\text{long}e} &= \left[\, \delta_{\omega 0} \;\; \delta_{E0} \,\right]^{\mathrm{T}}, \\ x_{\text{lat}e} &= \left[\, 0 \;\; 0 \;\; 0 \;\; 0 \;\; \psi_0 \,\right]^T, \\ u_{\text{lat}e} &= \left[\, \delta_{A0} \;\; \delta_{R0} \,\right]^T; \end{aligned}$$

where ψ_0 can take any arbitrary value. If Eqns. (46) are solved numerically, it can be found that the equilibrium values can be parametrized by $\sigma = \left[\, V_{T0} \;\; h_0 \,\right]^{\mathrm{T}}$ or $\sigma = \left[\, \alpha_0 \;\; h_0 \,\right]^{\mathrm{T}}$. This means that when V_{T0} and h_0 are given, α_0 and h_0 can be found, and vice versa. Thus, it is true that $x_{\text{long}e} = x_{\text{long}e}(\sigma)$, $u_{\text{long}e} = u_{\text{long}e}(\sigma)$, $x_{\text{lat}e} = x_{\text{lat}e}(\sigma)$ and $u_{\text{lat}e} = u_{\text{lat}e}(\sigma)$. Every equilibrium point parametrized by σ leads to a Jacobian–linearized model also parametrized by σ

$$\begin{aligned} \dot{x}_{\text{long}\delta} &= A_{\text{long}}(\sigma)\, x_{\text{long}\delta} + B_{\text{long}}(\sigma)\, u_{\text{long}\delta}, \\ \dot{x}_{\text{lat}\delta} &= A_{\text{lat}}(\sigma)\, x_{\text{lat}\delta} + B_{\text{lat}}(\sigma)\, u_{\text{lat}\delta}; \end{aligned} \tag{47}$$

where

$$\begin{aligned} x_{\text{long}\delta} = x_{\text{long}} - x_{\text{long}e}(\sigma), & \; u_{\text{long}\delta} = u_{\text{long}} - u_{\text{long}e}(\sigma), \\ x_{\text{lat}\delta} = x_{\text{lat}} - x_{\text{lat}e}(\sigma), & \; u_{\text{lat}\delta} = u_{\text{lat}} - u_{\text{lat}e}(\sigma). \end{aligned}$$

If the Jacobians in Eqn. (47) can be found numerically, *e.g.* using fourth order centered differences, their general from is given by

$$A_{\text{long}}(\sigma)=\begin{bmatrix} a_{\text{long}11}(\sigma) & a_{\text{long}12}(\sigma) & a_{\text{long}13}(\sigma) & 0 & 0\\ a_{\text{long}21}(\sigma) & a_{\text{long}22}(\sigma) & a_{\text{long}23}(\sigma) & 0 & 0\\ a_{\text{long}31}(\sigma) & a_{\text{long}32}(\sigma) & a_{\text{long}33}(\sigma) & 0 & 0\\ 0 & 0 & 1 & 0 & 0\\ 0 & a_{\text{long}52}(\sigma) & 0 & a_{\text{long}54}(\sigma) & 0 \end{bmatrix},$$
$$B_{\text{long}}(\sigma)=\begin{bmatrix} b_{\text{long}11}(\sigma) & b_{\text{long}12}(\sigma)\\ b_{\text{long}21}(\sigma) & b_{\text{long}22}(\sigma)\\ 0 & b_{\text{long}32}(\sigma)\\ 0 & 0\\ 0 & 0 \end{bmatrix},$$
$$A_{\text{lat}}(\sigma)=\begin{bmatrix} a_{\text{lat}11}(\sigma) & a_{\text{lat}12}(\sigma) & a_{\text{lat}13}(\sigma) & a_{\text{lat}14}(\sigma) & 0\\ a_{\text{lat}21}(\sigma) & a_{\text{lat}22}(\sigma) & a_{\text{lat}23}(\sigma) & 0 & 0\\ a_{\text{lat}31}(\sigma) & a_{\text{lat}32}(\sigma) & a_{\text{lat}33}(\sigma) & 0 & 0\\ 0 & 0 & a_{\text{lat}43}(\sigma) & 0 & 0\\ 0 & 0 & 0 & a_{\text{lat}54}(\sigma) & 0 \end{bmatrix},$$
$$B_{\text{lat}}(\sigma)=\begin{bmatrix} b_{\text{lat}11}(\sigma) & b_{\text{lat}12}(\sigma)\\ b_{\text{lat}21}(\sigma) & b_{\text{lat}22}(\sigma)\\ b_{\text{lat}31}(\sigma) & b_{\text{lat}32}(\sigma)\\ 0 & 0\\ 0 & 0 \end{bmatrix}; \tag{48}$$

and if they are parametrized by $\sigma=\left[\,\alpha_0\ h_0\,\right]^{\mathrm{T}}$ an illustration of A_{long} is shown in Fig. 3 (solid surface). It is obvious that the dependence on σ of the Jacobians (Eqns. (48)) is in general nonlinear, so the affine condition in Eqn. (2) does not hold. An alternative, is to find a static least-square-sense approximation [17] of the surfaces defined by the elements in Eqn. (48), so they can fit in an affine structure. A possibility to do that is using the two parameter structure

$$\begin{aligned} \mathrm{A}(\sigma) &= M_{A0}+\alpha_0 M_{A\alpha}+h_0 M_{Ah},\\ \mathrm{B}(\sigma) &= M_{B0}+\alpha_0 M_{B\alpha}+h_0 M_{Bh}; \end{aligned}$$

for each matrix in Eq. (48). This approximation is depicted in Fig. 3 (mesh). Moreover, a better approximation is using a three-parameter option where one of the parameters is the square of α

$$\begin{aligned} \mathrm{A}(\sigma) &= M_{A0}+\sigma_1 M_{A\alpha}+\sigma_2 M_{A\alpha2}+\sigma_3 A_h\\ &= M_{A0}+\alpha_0 M_{A\alpha}+\alpha_0^2 M_{A\alpha2}+h_0 M_{Ah},\\ \mathrm{B}(\sigma) &= M_{B0}+\sigma_1 M_{B\alpha}+\sigma_2 M_{B\alpha2}+\sigma_3 B_h\\ &= M_{B0}+\alpha_0 M_{B\alpha}+\alpha_0^2 M_{B\alpha2}+h_0 M_{Bh}. \end{aligned}$$

Since the functions α and α^2 are linearly independent, data of α_0 will be independent of α_0^2. In this last case the parameter polytope Θ is defined by the region

$$\Theta=\Big\{\sigma=\left[\,\sigma_1\ \sigma_2\ \sigma_3\,\right]^{\mathrm{T}}:\sigma_1\in[\alpha_{0\min},\alpha_{0\max}],\ \sigma_2\in[\alpha_{0\min}^2,\alpha_{0\max}^2],\sigma_3\in[h_{0\min},h_{0\max}]\Big\}. \tag{49}$$

CONTROLLER DESIGN

The design goals and the controller structure are defined by choosing the measured variables y, the controlled variables z and the exogenous variables w. The set of controlled and measured variables define which mapping norm is to be optimized, because the control goal is to minimize the $\mathcal{H}_\infty$ norm of the $w\rightarrow z$ mapping. The exogenous variables are the setpoints and the output disturbances; the controlled variables are the errors, the error integrals, the part of the state vector not covered in the errors and the control inputs; the measured variables, *i.e.* the variables used by the controller are given by the errors, are the error integrals and the part of the state not covered by the error.

Since the longitudinal and lateral controllers are designed from the uncoupled models, each controller is designed separately. Then, for the longitudinal mode the variables are

$$\begin{aligned} w &= \left[\,V_{Td}\ h_d \middle| d_{V_T}\ d_h\,\right]^{\mathrm{T}},\\ z &= \left[\,V_{Td}-V_T\ \ h_d-h \middle| \int V_{Td}-V_T\ \int h_d-h \middle| -\alpha\ -q\ -\theta \middle| \delta_\omega\ \delta_E\,\right]^{\mathrm{T}},\\ y &= \left[\,V_{Td}-V_T\ \ h_d-h \middle| \int V_{Td}-V_T\ \int h_d-h \middle| -\alpha\ -q\ -\theta\,\right]^{\mathrm{T}}; \end{aligned} \tag{50}$$

and for the lateral mode the variables are

$$\begin{aligned} w &= \left[\,\psi_d \middle| d_\psi\,\right]^{\mathrm{T}},\\ z &= \left[\,\psi_d-\psi \middle| \int \psi_d-\psi \middle| -\beta\ -p\ -r\ -\phi \middle| \delta_A\ \delta_R\,\right]^{\mathrm{T}},\\ y &= \left[\,\psi_d-\psi \middle| \int \psi_d-\psi \middle| -\beta\ -p\ -r\ -\phi\,\right]^{\mathrm{T}} \end{aligned} \tag{51}$$

The variables' selection looks for a trade-off between error, state and control effort minimization in an $\mathcal{H}_\infty$ sense. This design problem is solved by calculating the LMIs proposed previously, using Matlab®'s *LMI Control Toolbox*, since it has ready-to-use LMI solving and $\mathcal{H}_\infty$ robust control synthesis tools [14, 15].

CONTROLLER IMPLEMENTATION

The controller implementation requires considering two main topics: the convex decomposition problem and the scheduling variables update. The first one defines the scheduling technique and the latter defines how the controller's gains change with changes in the plant's dynamics.

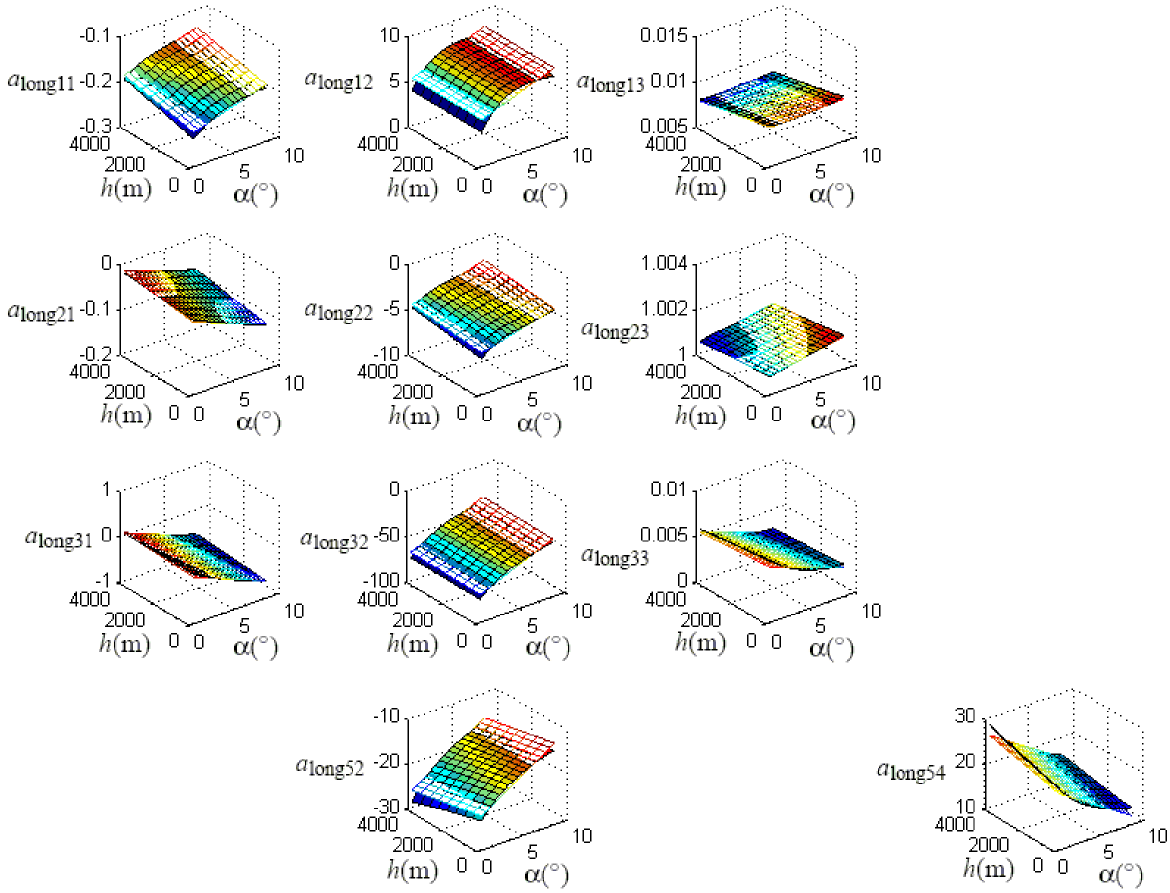

FIGURE 3. LONGITUDINAL MODEL: LPV (SOLID SURFACE), AFFINE APPROXIMATION (MESH)

Convex decomposition problem

When the synthesis problem is solved, the vertex controllers K_i are known. These vertex controller matrices define the LPV controller through the convex combination

$$K(\sigma) = \sum_{i=1}^{\mathrm{r}} \mu_i \mathrm{K}_i. \tag{52}$$

Equation (3) shows that there is a mapping between the convex coordinates μ_i and the parameter σ *i.e.* if all μ_i $(i = 1, \ldots, \mathrm{r})$ are known, a particular $\sigma \in \Theta$ is given.

The convex decomposition problem consists in finding an inverse of the mapping in Eqn. (3), *i.e.* for a given σ one have to find a set of μ_i $(i = 1, \ldots, \mathrm{r})$ satisfying Eqn. (3). The two-parameter case is shown in [9] and the convex coordinates are given by

$$\begin{gathered}\mu_1 = ab, \mu_2 = (1-a)\,b, \mu_3 = a\,(1-b)\,, \\ \mu_4 = (1-a)\,(1-b)\,;\end{gathered} \tag{53}$$

where

$$a = \frac{\sigma_1^{\max} - \sigma_1}{\sigma_1^{\max} - \sigma_1^{\min}}, \quad b = \frac{\sigma_2 - \sigma_2^{\min}}{\sigma_2^{\max} - \sigma_2^{\min}}.$$

A similar solution for the three-parameter case can be found. Then, the convex coordinates are given by

$$\begin{gathered}\mu_1 = abc, \mu_2 = (1-a)\,bc, \mu_3 = a\,(1-b)\,c, \\ \mu_4 = (1-a)\,(1-b)\,c, \mu_5 = ab\,(1-c)\,, \\ \mu_6 = (1-a)\,b\,(1-c)\,, \mu_7 = a\,(1-b)\,(1-c)\,, \\ \mu_8 = (1-a)\,(1-b)\,(1-c)\,;\end{gathered} \tag{54}$$

where

$$a = \frac{\sigma_1 - \sigma_1^{\min}}{\sigma_1^{\max} - \sigma_1^{\min}}, b = \frac{\sigma_2 - \sigma_2^{\min}}{\sigma_2^{\max} - \sigma_2^{\min}}, c = \frac{\sigma_3 - \sigma_3^{\min}}{\sigma_3^{\max} - \sigma_3^{\min}}.$$

Using Eqn. (53) or Eqn. (54), Eqn. (52) can be rewritten as

$$K(\sigma) = \sum_{i=1}^{r} \mu_i(\sigma) K_i;$$

where the scheduling mechanism is defined through this convex combination and updated through σ.

Scheduling variables

It is known that σ updates the controller. In previous sections σ was defined from steady–state values, and in the polytopic description was defined as $\sigma = \left[\, \alpha_0 \; h_0 \,\right]^{\mathrm{T}}$. But in order to update the controller, a measurable or known value related to these values must be chosen. Two possible choices are: using the actual measured or estimated value related to the variables, *i.e.* $\sigma = \left[\, \alpha \; h \,\right]^{\mathrm{T}}$; or using the setpoint value related to the variables, *i.e.* $\sigma = \left[\, \alpha_d \; h_d \,\right]^{\mathrm{T}}$. In the first case, the controller's gains change as fast as the variables change, so this is not a recommendable choice since the angle of attack suffers several changes during operation that may lead the non-linear closed-loop system to instability. In the second case, the controller's gains change as quickly as the setpoints change; this is a more plausible choice because in this case the setpoints's changes are smooth and rate-filtered.

The main reason to use the above mentioned choice for σ, is that the controller is designed from a parametrization of the family of linearized models. These models are good if the system is near a steady-state condition. Moreover, the controller works well if its gains match the appropriate steady-state condition, and choosing the instantaneous α instead of a setpoint could mislead the controller to a non-correspondent steady-state condition. This fact is treated theoretically in [18].

In order to implement the controller, σ is updated using the rule

$$\sigma = \left[\, \alpha_d(V_{Td}) \; h_d \,\right]^{\mathrm{T}},$$

where α_d is not directly a setpoint and V_{Td} is the desired velocity. The mapping $\alpha_d(V_{Td})$ is defined by the steady-state relation between these two variables.

SIMULATION RESULTS

The designed controllers are tested through numeric simulation of the complete model of the vehicle, Eqns. (21)-(29), and using a three-level hierarchical architecture. The highest level is a mission planner with a trajectory generator which gives a set of feasible waypoints, the mid-level is a guidance system that takes the waypoints and calculates filtered setpoints for the low-level controller. In the low-level, the designed $\mathcal{H}_\infty$ controller stabilizes the vehicle and follows the set-point changes manipulating the vehicle's control inputs.

The trajectory waypoints used in the controller test are resumed in Table 1 and illustrated in Fig. 4. In the mode column 1 = passthrough, 2 = cut and 3 = loiter; the North and East columns are objective-point coordinates in the passthrough and cut modes and center-point coordinates in the loiter mode; and in the turn radius column a positive radius means clockwise loiter and a negative one means counter-clockwise loiter.

The trajectory achieved using the $\mathcal{H}_\infty$ algorithm in the low-level controller is shown in Fig. 4, the time response of the controlled variables is shown in Fig. 5 and the control inputs behavior is shown in Fig. 6. These results show that an adequate system behavior can be achieved through the chosen control strategy, thus the controller can handle gradual smooth set-point changes given by the trajectory generator.

TABLE 1. WAYPOINTS

ID	Mod	North (m)	East (m)	Alt. (m)	Speed (km/h)	Rad. (m)	No. turns
1	1	100	0	1500	70	-	-
2	1	500	0	1500	75	-	-
3	1	1000	0	1500	70	-	-
4	3	1000	500	1500	70	500	1
5	1	1500	0	1500	70	-	-
6	1	2000	0	1550	70	-	-
7	3	2000	-500	1550	70	-500	1/2
8	1	1000	-1000	1500	70	-	-
9	2	500	-1000	1500	70	250	-
10	1	0	0	1500	70	-	-

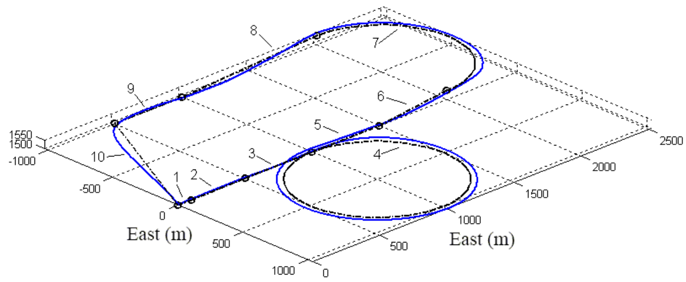

FIGURE 4. ACHIEVED TRAJECTORY

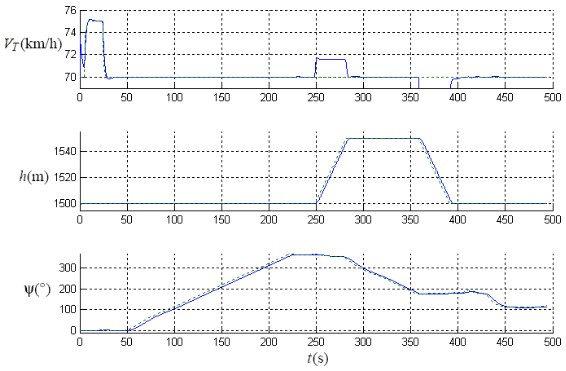

FIGURE 5. CONTROLLED VARIABLES: VELOCITY (TOP), ALTITUDE(MIDDLE) AND HEADING (BOTTOM)

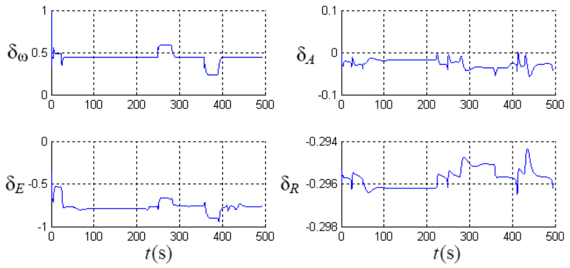

FIGURE 6. CONTROL INPUTS

CONCLUSIONS

This work addressed the design of a robust $\mathcal{H}_\infty$ controller for the low-level control of a fixed-wing unmanned aerial vehicle (UAV) based on an LPV polytopic approximation of the Jacobian linearization family.

The controller synthesis was made by using the Bounded Real Lemma, guaranteeing global quadratic stability for the LPV system with a unique Lyapunov function and $\mathcal{H}_\infty$ robust performance. The synthesis problem was expressed as a finite number of LMIs and solved numerically using available tools. The controller performance was evaluated through numeric simulation of the complete model of the vehicle, along with a guidance system that calculates appropriate setpoints for the $\mathcal{H}_\infty$ controller.

Simulation results showed that the controller regulates the vehicle's flight in a robust manner and smooths the controlled variables and the control inputs behavior, keeping the best possible performance in terms of error elimination, fast time response and trajectory tracking. The performance of the controller can be improved including some weights in the controlled outputs.

ACKNOWLEDGMENT

The authors gratefully acknowledge the partial financial support given by the Universidad Pontificia Bolivariana for the Master of Science studies of Juan A. Ramirez.

REFERENCES

[1] Vásquez, J. M., 2007. "Mechanical pre-design of an automatic system for power transmision lines inspection". Master's thesis, School of Engineering, Universidad Pontificia Bolivariana, Colombia.

[2] Múnera, D. A., 2005. "Design and integration of a modular system for navigation control of an unmanned vehicle". Master's thesis, School of Engineering, Universidad Pontificia Bolivariana, Colombia.

[3] Ortiz, P., 2008. "Mathematical model for a fixed-wing uav using parametric identification methods". Master's thesis, School of Engineering, Universidad Pontificia Bolivariana, Colombia.

[4] Zuluaga, C. A., 2007. "Simulation platform for autonomous vehicles". Master's thesis, School of Engineering, Universidad Pontificia Bolivariana, Colombia.

[5] Cardona, L., 2008. "Navigation system for unmanned vehicles". Master's thesis, School of Engineering, Universidad Pontificia Bolivariana, Colombia.

[6] Gutiérrez, L., 2004. "Adaptive mode transition control architecture with an application to unmannedaerial vehicles". PhD thesis, School of Electrical and Computer Engineering, Georgia Institute of Technology.

[7] Vachtsevanos, G., Tang, L., Drozeski, G., and Gutiérrez, L., 2005. "From mission planning to flight control of unmanned aerial vehicles: Strategiesand implementation tools". *Annual Reviews in Control*, ***29***, pp. 101 – 115.

[8] Gahinet, P., and Apkarian, P., 1994. "A lineal matrix inequality approach to $\mathcal{H}_\infty$ control". *Int. J. Robust and Nonlinear Control*, ***4***, pp. 421 – 448.

[9] Apkarian, P., Gahinet, P., and Becker, G., 1995. "Self-scheduled $\mathcal{H}_\infty$ control of linear parameter-varyingsystems: a design example". *Automatica*, ***31***, Sep., pp. 1251 – 1261.

[10] Apkarian, P., and Gahinet, P., 1995. "A convex characterization of gain-scheduled $\mathcal{H}_\infty$ controllers". *IEEE Transactions on Automatic Control*, ***5***, May, pp. 853 – 864.

[11] Kemin, Z., and Doyle, J., 1998. *Essentials of Robust Control*. Prentice Hall.

[12] Dullerud, G., and Paganini, F., 2000. *A Course in Robust Control Theory: A Convex Approach*. Springer.

[13] Rugh, W., and Shamma, J., 2000. "Research on gain scheduling". *Automatica*, ***36***, pp. 1401 – 1425.

[14] Gahinet, P., et al., 1994. "The LMI control toolbox". In Proceedings of the 33rd Conference on Decision and Control, pp. 2038 – 2041.

[15] Gahinet, P., et al., 1995. *LMI Control Toolbox for use with Matlab*. The MathWorks.

[16] Stevens, B., and Lewis, F., 2003. *Aircraft Control and Simulation*. J. Wiley.

[17] Åström, K. J., and Wittenmark, B., 1995. *Adaptive control*, 2nd ed. Addison – Wesley.

[18] Khalil, H., 2002. *Nonlinear Systems*, 3^{rd} ed. Prentice Hall.